The Cryosphere Discuss., 8, 4463–4495, 2014
www.the-cryosphere-discuss.net/8/4463/2014/
doi:10.5194/tcd-8-4463-2014

The Cryosphere
Discussions
Open Access

A conceptual model of cyclical glacier flow in overdeepenings

J. B. Turrin and R. R. Forster

University of Utah, Geography Department, Salt Lake City, UT, USA

Received: 29 July 2014 – Accepted: 29 July 2014 – Published: 12 August 2014

Correspondence to: J. B. Turrin (jturrin@hotmail.com)

Published by Copernicus Publications on behalf of the European Geosciences Union.

Abstract

A nearly four-decade, satellite-based velocity survey of the largest glaciers in the Alaska Range, Chugach Mountains, and the Wrangell Mountains of southern Alaska, spanning the early- to mid-1970s through the 2000s, reveals nine pulsing glaciers: Capps, Copper, Eldridge, Kahiltna, Matanuska, Nabesna, Nizina, Ruth, and Sanford glaciers. The pulses increase velocity by up to 2449 % (Capps Glacier) or as little as 77 % (Nabesna Glacier), with velocity increases for the other glaciers in the range of 100–250 %. The pulses may last from between six years (Copper Glacier) to 12 years (Nizina Glacier) and consist of a multi-year acceleration phase followed by a multi-year deceleration phase during which significant portions of each glacier move en masse. The segments of each glacier affected by the pulses may be anywhere from 14 km (Sanford Glacier) to 36 km (Nabesna Glacier) in length and occur where the glaciers are either laterally constricted or joined by a major tributary, and the surface slopes at these locations are very shallow, 1–2°, suggesting the pulses occur where the glaciers are overdeepened. A conceptual model to explain the cyclical behavior of these pulsing glaciers is presented that incorporates the effects of glaciohydraulic supercooling, glacier dynamics, surface ablation, and subglacial sediment erosion, deposition, and deformation in overdeepenings.

1 Introduction

Mayo (1978) defined a glacier pulse as periodic unstable flow lesser in magnitude than surge-type behavior. We further define a glacier pulse as a type of dynamic behavior characterized by a multi-year acceleration phase in which the glacier progressively increases its velocity due to deformation of a subglacial till, immediately followed by a multi-year deceleration phase during which the glacier progressively slows as the till consolidates. This nomenclature is borrowed from the three phases of Svalbard-type surges, which have acceleration, deceleration, and quiescent phases (Murray et al., 2003), and which also accelerate due to till deformation. Pulses are cyclical in nature, as has been found on Black Rapids Glacier (Nolan, 2003), Trapridge Glacier (Frappé and Clarke, 2007), and Ruth Glacier (Turrin et al., 2014), with the cycles lasting from four to 12 years. As discussed by Turrin et al. (2014), and based on theory by Fowler et al. (2001), the till at the base of a pulsing glacier is perennially temperate, not frozen, which allows almost instantaneous transfer of shear stresses. So, when a till dilates (due to high basal water pressure) and can no longer support shear stress, the stress is immediately transferred to nearby locations that may also be near their threshold of failure and which will also dilate, deform, and again transfer the stress elsewhere. This process results in a cascade of till failure and stress transfer beneath a glacier that Nolan (2003) describes as activation waves. These activation waves move so rapidly beneath a glacier that the activated portion of the glacier slumps forward all at once, rather than forming a kinematic wave at the leading edge of the activation wave as it travels down glacier. De-pressurization of the subglacial drainage system and consolidation of the till brings an end to a pulse. Again, this appears to happen without formation of a kinematic wave, so deactivation of the till must occur rapidly as well. Therefore, pulses are characterized by a spatio-temporal velocity signature in which a portion of a glacier accelerates and then decelerates en masse; no wave front is evident at the glacier surface as might be seen during a surge (e.g. Bering Glacier, Turrin et al., 2013). Instead, the surface of pulsing glaciers is characterized by wavy medial moraines, large-scale wavy foliation, boudinage and potholes (Mayo, 1978), each a result of pulses repeatedly compressing and extending the ice.

Pulses produce increased basal motion via a change in the state of a subglacial till from consolidated to dilated (and subsequent deformation), while surges increase basal motion via slip at the ice/bed interface, and involve a transformation of the subglacial drainage system from low-pressure, fast flow in channels to high-pressure slow flow through distributed cavities (Kamb et al., 1985). The rate at which these subglacial changes occur determines whether a kinematic wave forms, or not. The slower process of re-shaping the drainage system beneath a glacier results in the formation of

TCD
8, 4463–4495, 2014

a kinematic wave during a surge (e.g. Turrin et al., 2013), while the faster process of till dilation precludes the formation of a kinematic wave. Both processes are cyclical. While a surge cycle is dependent upon the varying rates of ice accumulation and ablation (which are driven by climate) to achieve a longitudinal surface profile that is unstable, the mechanism that causes periodicity in glacier pulses is unknown. Nolan (2003) suggests at the end of a pulse the subglacial till may be incompletely drained and hence only partially consolidated, leaving it primed for another pulse when subglacial water pressure rises again. This idea does not provide a mechanism to fully explain why periodicity exists on pulsing glaciers; it merely suggests a scenario in which a till might easily deform again. A complete answer as to why periodicity exists on pulsing glaciers is lacking. Therefore, the aim of this study is to provide a conceptual model to explain the oscillatory nature of glacier pulses, based on observations and previous theory.

2 Study region

To construct a theory that explains the cyclical behavior of pulsing glaciers, glaciers that have recently pulsed must be identified, their dynamic behavior studied, and their common characteristics analyzed. To help accomplish these tasks, velocity fields of the 90 largest glaciers in the Alaska Range, Chugach Mountains, and Wrangell Mountains were produced from the 1970s through the 2000s to identify glacier pulses and their common traits. Pulsing glaciers were identified by their spatio-temporal velocity signature consisting of a multi-year acceleration phase, followed by a multi-year deceleration phase in which a significant portion of the ablation zone moved en masse. Nine glaciers were found to have experienced pulses within the past four decades, they are: Capps, Copper, Eldridge, Kahiltna, Matanuska, Nabesna, Nizina, Ruth, and Sanford glaciers (Fig. 1). For brevity we will focus primarily on Nizina Glacier in this article to illustrate the typical pulsing behavior revealed by this study. The reader is referred to Turrin et al. (2014) for a complete examination of the pulses found on Ruth Glacier and the online Supplement for figures and results for the other seven glaciers. Of these nine

TCD
8, 4463–4495, 2014

glaciers, Mayo (1978) specifically lists five of them, Capps, Kahiltna, Nizina, Ruth, and Sanford glaciers, as pulse-type glaciers. The other four glaciers are not mentioned, but Mayo (1978) counted approximately 140 pulse-type glaciers in southern Alaska and did not provide all their names. Post (1969) lists the North Fork of Eldridge Glacier as surge-type, but not the main branch, and he lists Capps Glacier as possibly being of surge-type.

Nizina Glacier (Fig. 2) is located in the Wrangell Mountains and is approximately 33 km in length and 2.5 km wide in the ablation zone. Its accumulation zone consists of two large lobes that merge between 5 and 10 km to form the main glacier trunk, and a small lobe that contributes ice to the main trunk along the southern margin near 12 km. Nizina Glacier is joined by Rohn Glacier near 22 km. Rohn Glacier is roughly equal in size to Nizina Glacier but moves slower, so it experiences greater surface lowering due to ablation, greater sediment retention on its surface and therefore has a lower albedo overall. Nizina Glacier is more active than Rohn Glacier and consequently transports its ice further down valley, forming most of the terminus of the combined glacier system; while the ice of Rohn Glacier completely ablates by 28 km. Nizina Glacier is embedded with numerous prominent linear medial moraines that become slightly around 28 km indicating past pulsing behavior. Nizina and Rohn glaciers are underlain by two different formations of lava and four different formations of sedimentary bedrock, labeled as QTw, Trn, Kl, Ku, Pl, and Ph in Fig. 2, respectively (Richter et al., 2006).

3 Methods

COSI-Corr feature tracking software (Leprince et al., 2007) was used to produce velocity fields in conjunction with Landsat Multispectral Scanner System (MSS), Thematic Mapper (TM), Enhanced Thematic Mapper Plus (ETM+), and Operational Land Imager (OLI) satellite imagery. See Table 1 for the date and sensor of the images used to produce the velocity fields for glaciers of the Wrangell Mountains. Also see Tables S1

TCD
8, 4463–4495, 2014

J. B. Turrin and R. R. Forster

through S3 in the Supplement for the date and sensor of images covering the Alaska Range and Chugach Mountains. When two Landsat-7 ETM+ images with scan-line voids were matched, which occurs for ETM+ images acquired after the May 2003 failure of the scan-line correction system, then orientation images were produced (Fitch et al., 2002) prior to insertion into COSI-Corr. The individual displacement measurements produced by COSI-Corr were processed to create velocity fields in the manner described by Turrin et al. (2014). The exception to this processing chain involves the use of OLI images which have a 12 bit quantization (4096 distinct brightness values may be recorded by the sensor for each optical band); whereas previous Landsat TM and ETM+ images have 8 bit quantization (256 distinct brightness values may be recorded). To rectify this difference, OLI images were re-quantized to eight bits prior to insertion into COSI-Corr. The final product is a time-series of velocity rasters that allows identification of those glaciers which have recently pulsed and their common characteristics.

The accuracy of the velocity fields depends upon the precision of the feature tracking algorithm used to produce the displacement measurements and how well the two images being matched are aligned. COSI-Corr has been shown to have a measurement error of ±0.08 pixel (±1.2 m) for 15 m ETM+ panchromatic imagery (Heid and Kääb, 2012). If we extrapolate this same level of precision to 30 m imagery the expected error is ±2.4 m, and for 60 m imagery it is ±4.8 m. Turrin et al. (2014) showed the average misalignment between two MSS images with 60 m spatial resolution is 0.25 ± 0.07 pixel, or 14.1 ± 4.2 m, and for 30 m TM and ETM+ image pairs the average misalignment is 0.15 ± 0.07 pixel, or 4.9 ± 2.6 m, after removal of the systematic error. Only one OLI image was used in this study (see Table 1) and its geolocation error is 0.15 pixel (4.6 m), as listed in the metadata accompanying the image by the US Geological Survey. This value is comparable to the average value of 0.16 ± 0.04 pixel of geolocation error for TM and ETM+ images found by Turrin et al. (2014), so we expect the velocity field produced using the OLI image to have an error similar in magnitude to those produced using TM and ETM+ images. The total error in the velocity fields is

TCD
8, 4463–4495, 2014

estimated from the precision of COSI-Corr and the final image misalignment using the root sum of squares method, because these variables are independent of one another. For 30 m TM, ETM+, and OLI imagery the error is estimated to be 5.1 m (0.17 pixel), and for 60 m MSS imagery the error is estimated to be 15.7 m (0.26 pixel).

The bedrock formations that underlie each of the nine glaciers were taken from either a US Geological Survey Open-File Report (Wilson et al., 1998) or a US Geological Survey Scientific Investigations Map (Richter et al., 2006). These maps are compilations and re-interpretations of many published and unpublished works and provide the geologic structure and bedrock lithology of each mountain range at a level appropriate for this study. Subsets of these geologic maps were georeferenced to a Landsat image by manually picking tie-points between the map and the satellite image. During the georeferencing routine the geologic maps were also resampled to 30 m spatial resolution to match the Landsat image. The subsequent location error of the georeferenced geologic maps is estimated to be up to 5 pixels (150 m) in some locations, but less in most locations. Using the georeferenced geologic maps as a backdrop, the bedrock formations underlying each glacier were outlined and overlaid upon the Landsat images (see Fig. 2 and also Figs. S1, S5, S9, S13, S17, S21, and S25 in the Supplement). Each bedrock formation is labeled using the same stratigraphic symbol as in the source map.

4 Results for Nizina Glacier

The velocity fields (Fig. 3) and velocity time-series (Fig. 4) for Nizina Glacier show that since 1996 it has experienced one complete pulse cycle and is currently in the acceleration phase of a second pulse. From 1998 to 2002 Nizina Glacier slowly increased in velocity from 21.5 to 66.0 m a^{-1} at 24 km (Fig. 4), then from 2002 to 2004 the glacier accelerated significantly, increasing its velocity to a peak value of 221.1 m a^{-1} at 24 km, a 235 % increase. The glacier decelerated just as rapidly, with its velocity decreasing to 55.5 m a^{-1} by 2006, and then further decreasing to 35.0 m a^{-1} in 2009. The complete pulse cycle, from one local velocity minimum to the next, 1998 to 2009, lasted eleven years. Since 2009 Nizina Glacier has been steadily accelerating in a manner very similar to the acceleration phase of the 1998–2009 pulse. All the ice from 12 km to the terminus at 30 km, an 18 km span, is affected by the pulses, with the ice accelerating and then decelerating en masse (Fig. 5a and b), but Rohn Glacier, which converges with Nizina Glacier at 22 km (see Fig. 2), does not pulse (see Fig. 3). However, the convergence of the slower-moving ice of Rohn Glacier does affect Nizina Glacier, as indicated by local velocity minima in the velocity profiles (Fig. 5a and b) at 22 km. At, or near, 26 km several velocity profiles (02/03, 03/04, 04/05, 05/06, 11/12) show a peak velocity. This location coincides with a transition in bedrock geology from basalt lava (Trn) to sedimentary bedrock (Kl, Ku, and Pl). From roughly 14 to 25 km the surface slope of Nizina Glacier is $< 2^{\circ}$, with much of this stretch dipping even more gently at an angle of 1.5°, by 26–27 km the surface slope has increased to 2°, coinciding with the velocity maxima seen in the velocity profiles.

5 Discussion

Sections 5.1 through 5.4 discuss accepted or proposed glaciologic theory concerning the characteristics of pulsing glaciers, overdeepenings, basal hydrology, glaciohydraulic supercooling, and till deposition, deformation and erosion. These processes are then linked in a chain of events to explain why pulses are cyclical in Sect. 5.5.

5.1 Physical characteristics of pulsing glaciers

By examining the spatio-temporal patterns of velocity and the physical attributes of the nine glaciers in this study, it is possible to identify some common characteristics of pulsing glaciers. The part of the glaciers in which the spatio-temporal pattern of velocity indicates pulsing behavior (i.e. a multi-year acceleration phase followed by a multi-year deceleration phase, and the lack of a kinematic wave) is always located where the ice surface has the shallowest slope, which is generally in the range of 1–2°. The exception to this is Nabesna Glacier which has a surface slope of 2° where the pulse most strongly affected the glacier, but a shallower slope of 1° up glacier, near 30 km where the effect of the pulse diminishes (see Supplement, Figs. S21–S23). The pulses of Capps, Copper, Kahiltna, Nabesna, and Ruth glaciers all occur where the glacier either increases in width after exiting a constricted area (Ruth, Kahiltna), or after exiting its confining valley (Capps), or within its confining valley (Copper, Nabesna). In all these instances, the constrictions appear to be controlled by the underlying bedrock lithology and involve a transition from crystalline bedrock, such as granite or basalt, to sedimentary bedrock. Again, the exception is Nabesna Glacier, which involves a transition from a mix of lava and sedimentary bedrock to strictly lava (see Supplement, Fig. S21). The pulses of Eldridge, Matanuska, Nizina, and Sanford glaciers all occur where one or more tributary glaciers merge with the main ice trunk (see Fig. 1 and also Figs. S1, S13, S25). In each case the tributary glaciers are moving slowly compared to the main trunks they join, and in each case the tributary glaciers are of noteworthy size and likely contributed significant mass to the main trunks during previous ice ages. Although there are some transitions in bedrock lithology that coincide with the union of tributary glaciers and their main trunks (Eldridge, Nizina), it does not appear that the location of the each glacier confluence is controlled by the underlying bedrock lithology.

5.2 Formation and characteristics of overdeepenings

A glacial overdeepening is a bowl-shaped depression beneath a glacier with a bottom that is lower in elevation than the glacier base immediately down valley; thus, the glacier is "overly deep" at this location. Overdeepenings typically have steeply inclined headwalls at their up glacier extents and gently inclined slopes at their down valley extents that dip opposite in direction of the glacier surface slope (Hooke, 2005); thus, the down valley slope is often referred to as the adverse slope. Overdeepenings can be found in cirques, at glacier confluences, valley constrictions, beneath glacier termini, or where a change in geologic structure or lithology occurs (Cook and Swift, 2012). In each of these cases, the overdeepening is formed due to increased erosion beneath

TCD
8, 4463–4495, 2014

J. B. Turrin and R. R. Forster

the glacier, caused either by an increase in ice flux or a decrease in the ability of the bedrock to withstand erosive forces. The circumstances listed herein that can lead to the formation of overdeepenings are common in alpine environs; therefore, overdeepenings are common and can be found at all elevations in the glacial landscape (Hooke, 2005).

An overdeepening begins as a basal step beneath a glacier, for instance, just down glacier from where a tributary merges with a main glacier trunk. The increase in ice flux at the confluence of the two ice masses causes increased erosion at the glacier base, forming a step (Penck, 1905). The convex shape of the basal step causes extension of the ice surface as the glacier flows over it, resulting in crevasses above the step. The crevasses act as preferential waterways, directing melt water to the head of the step, increasing basal sliding locally at the base of the headwall of the step, thus further increasing erosion there. Increased erosion at the base of the headwall increases its slope and enhances its convex shape, thus increasing ice surface extension and crevassing above it (Hooke, 2005). This positive feedback promotes transformation of basal steps into overdeepenings. The ice surface above overdeepenings tends towards shallow slopes because the ice velocity is greater in the overdeepening relative to down glacier, due to basal slip and till deformation. The increased velocity causes ice extension within the overdeepening and ice compression immediately down glacier that reduces the ice surface slope locally (Cook and Swift, 2012).

Glacier pulses are observed to occur in the same type of locations in which glacier overdeepenings form (at glacier confluences, valley restrictions, or changes in bedrock lithology), and overdeepenings are known to have flat ice surface slopes, just as observed at the locations where pulses occur. Consequently, it is concluded that pulses occur where glaciers are overdeepened. There is some field evidence to show a few of the glaciers mentioned above are overdeepened in the location of the pulses. There is a single ice depth measurement of Ruth Glacier within the Great Gorge via seismic methods (unpublished data by K. Echelmeyer) that found the ice to be up to 1150 m thick in 1983. As Ward et al. (2012) note, ice this thick places the bottom of the Great

Gorge at approximately the same elevation as the terminus, nearly 40 km further down valley. This strongly suggests the Great Gorge of Ruth Glacier is overdeepened. As Turrin et al. (2014) showed, the pulses of Ruth Glacier occur immediately below the Great Gorge and probably originated there, but the velocity fields could not be extended into the gorge due to lack of trackable features. The ice thickness of Capps Glacier was measured using a monopulse ice-radar (March et al., 1997). It was found to be between 700 and 800 m thick in its main trunk between 20 and 27 km, where the glacier is most narrow, before it spreads laterally and forms a piedmont lobe. The surface elevation along this part of the glacier is between 600 and 800 m a.s.l. and the glacier terminus is approximately 150 m a.s.l. (see Supplement, Fig. S11). Therefore, the base of the glacier is at, or below, sea level between 20 and 27 km and definitely overdeepened there. In fact, the data suggest the overdeepening extends well into the piedmont lobe to at least 35 km, because the ice thickness is still greater than the surface elevation there, indicating the glacier base resides below sea level and must be overdeepened; this is the same portion of Capps Glacier that pulsed.

5.3 Basal hydrology and supercooling in overdeepenings

The subglacial hydraulic system beneath overdeepenings is a distributed-cavity system with high water pressure and slow flow that transitions to a channelized system with faster flow at the distal parts of the adverse slope (Alley et al., 2003; Hooke, 2005; Creyts et al., 2013). High water pressures have been observed via field studies of overdeepenings on Storglaciären, Sweden (Jansson, 1996) and Washmawapta Glacier, British Columbia (Dow et al., 2011), and have also been predicted by numerical modeling (Creyts et al., 2013). The high water pressure beneath an overdeepening is a result of constriction of the drainage channels along the adverse slope due to glaciohydraulic supercooling. Supercooling of subglacial water occurs within overdeepenings due to the increased ice thickness there depressing the pressure-melting point (at a rate of $-0.001\,^{\circ}\mathrm{C\,m^{-1}}$), which allows subglacial water to remain liquid below $0\,^{\circ}\mathrm{C}$. As the supercooled water traverses the adverse slope to exit the overdeepening, the

TCD
8, 4463–4495, 2014

A conceptual model of cyclical glacier flow in overdeepenings

J. B. Turrin and R. R. Forster

glacier thins along the slope and the pressure-melting point rises faster than the water can warm via viscous heating, so the water freezes onto the walls of the drainage channels, constricting them, or clogging them with frazil ice (ice platelets). Consequently, the water pressure rises and water is forced to spread laterally in the distributed-cavity system within the overdeepening (Alley et al., 2003; Hooke, 2005).

Whether the supercooled water actually freezes as it traverses the adverse slope, or not, depends upon the rate at which the pressure-melting point rises along the adverse slope, which in turn is determined by the ratio of the angle of the adverse slope to the angle of the ice surface slope. The supercooling threshold is defined as the critical angle of the adverse slope such that water moving along it will freeze. Hooke (1989) estimated the supercooling threshold to be between 1.5 and 2.0 times the surface slope, and Clarke (2005) estimated it to be between 1.3 and 1.6 times the surface slope. So, if the adverse slope is approximately 1.3 to 2.0 times steeper than the ice surface slope directly above, water will freeze in its subglacial channels rather than exiting the overdeepening. Based on these supercooling threshold values and the surface slopes of the nine pulsing glaciers studied here (see Supplement Figs. S3, S7, S11, S15, S19, S23, and S27), the adverse slopes necessary for supercooling to occur range from 1.9–3.0° for Kahiltna, Ruth, and Nizina glaciers, 2.6–4.0° for Capps, Eldridge, Matanuska, Nabesna, and Sanford glaciers, and from 3.9–6.0° for Copper Glacier. All of these scenarios require only gently inclined adverse slopes (only twice the surface slope, or less), suggesting the supercooling condition is easily met. Evidence for supercooling, such as frazil ice and ice growth around subglacial discharge vents, has been found on Matanuska (Evenson et al., 1999a), Malaspina, and Bering glaciers in Alaska (Evenson et al., 1999b), and Skeidaràrjökull, Skaftafellsjökull, and Kviarjökull, which are outlet glaciers of the Vatnajökull icecap, Iceland (Evenson et al., 2001), and evidence for constricted flow in an overdeepening has been found on Storglaciären, Sweden (Hooke and Pohjola, 1994) by the slow movement of tracer dyes through cavities beneath the glacier, observed via boreholes drilled into the base of the overdeepening.

5.4 Till deposition, deformation, and erosion

As glaciohydraulic supercooling causes subglacial drainage channels along an adverse slope to become constricted, thereby elevating water pressure in the distributed-cavity system within the overdeepening, the hydraulic gradient within the overdeepening decreases. The reduced gradient results in slower water flow such that sediment is no longer evacuated from the overdeepening; instead, it is deposited as a subglacial till. Thus, the overdeepening is transformed from an area of sediment erosion and transportation, to one of sediment deposition (Alley et al., 2003). The till will accumulate until the rate of down glacier sediment transport by deformation and entrainment within the ice is equal to the rate of erosion. Eventually, the till layer becomes thick enough to protect the bedrock beneath the overdeepening and adverse slope from further erosion, allowing erosion to concentrate at the headwall (Hooke, 2005).

Water pressure within an overdeepening can approach flotation levels, indicating that the weight of the overlying ice is supported by the water pressure, thus the effective pressure upon the till is zero. When this occurs, the till dilates (Willis, 1995) because it is no longer being compacted by the weight of the overlying glacier. A dilated till cannot support the shear stress between the overlying glacier and underlying bedrock, so the till deforms. Till deformation allows the glacier to accelerate locally, transferring shear stress to the immediate surroundings, and assuming the till in the immediate neighborhood is at or near its deformation threshold (due to high water pressure), these areas also deform and allow ice acceleration. The result is a cascade of till failure, ice acceleration, and stress transfer that activates more and more distant areas within the overdeepening (Truffer et al., 2000; Nolan, 2003; Frappé and Clarke, 2007); thus, a pulse begins.

Alley et al. (2003) proposed a theory of subglacial sediment deposition and erosion within overdeepenings that promotes equilibrium between the two processes. The theory is based upon field work performed mostly on the terminus of Matanuska Glacier where the ice has overridden unlithified sediment and an overdeepening exists (Alley

TCD
8, 4463–4495, 2014

J. B. Turrin and R. R. Forster

et al., 1998; Lawson et al., 1998). As sediment accumulates in the overdeepening, the angle of the adverse slope is reduced, changing the ratio of the adverse slope to the ice surface slope and eventually halting supercooling, because the supercooling threshold is no longer surpassed. Once supercooling ceases, the drainage pathways along the adverse slope can open because the water no longer freezes, there is sufficient viscous heating to keep the water liquid and to melt channel walls and keep them open and expand them. The expanded channelized hydraulic system sufficiently drains the deeper parts of the overdeepening to reduce water pressure there and cause the till to consolidate. The increased water flow begins the process of sediment erosion and transport again. Over time, enough sediment is evacuated that the angle between the adverse slope and surface slope is increased again to the supercooling threshold. Thus, sediment deposition and erosion work in tandem to continually arrange the longitudinal profile of an overdeepening to be at or near the supercooling threshold (Alley et al., 2003). Results from numerical modeling seem to confirm this theory. Creyts et al. (2013) used a one-dimensional model to simulate water flow and sediment transport through an overdeepening. When the model is forced with a constant basal water discharge, or a diurnally varying basal water discharge, the results indicate that if the angle of the adverse slope is less than the supercooling threshold, sediment deposition occurs in the overdeepening and along the adverse slope, as predicted by Alley et al. (2003). Alternatively, if the angle of the adverse slope is at the supercooling threshold, then sediment deposition occurs in the overdeepened area and along most of the adverse slope. Maximum deposition occurs where the adverse slope begins and tapers along the slope until there is minor erosion at its most distal part; the net effect is to reduce the overall angle of the adverse slope and cause supercooling to cease, also as predicted by Alley et al. (2003).

5.5 A conceptual model for cyclical pulses

The theory presented by Alley et al. (2003) for stabilization of the basal longitudinal profile of overdeepened glaciers at the supercooling threshold (summarized above) is for overdeepenings carved into unlithified sediment near the glacier terminus, where ice velocity is slowest and dynamic effects may be ignored. The pulses observed in this study and on Ruth Glacier (Turrin et al., 2014) occur in the mid- to upper ablation zone where the glaciers are moving rapidly compared to their termini, so dynamic effects must be accounted for. Presented below is a conceptual model to explain the cyclical dynamic behavior of these pulsing glaciers that incorporates the theory of Alley et al. (2003) and which also includes the effects of glacier dynamics.

1. Begin with an overdeepening that contains a consolidated till within its deepest parts and along the adverse slope (Fig. 6a, profile view), a distributed-cavity drainage system along much of the overdeepening and a channelized drainage system along part of the adverse slope (Fig. 6a, plan view), and a ratio of adverse slope to ice surface slope at the supercooling threshold. Assume effective pressure is greater than zero, there is no till deformation and the glacier is in between pulses, so ice motion is relatively slow. These are the initial conditions, prior to the beginning of a pulse.

2. Supercooling causes the channelized drainage system along the adverse slope to become constricted (Fig. 6b, plan view) by freezing of water as it exits the overdeepening. This causes high water pressure in the distributed-cavity drainage system that in turn causes the till to dilate and deform. The resulting shear strain in the till allows the glacier to accelerate, beginning a pulse. Transfer of shear stress allows the area of till failure beneath the glacier to expand; accelerating the glacier further. This is the acceleration phase of a pulse. As the glacier accelerates, the increased compressive strain rate along the adverse slope causes ice to thicken there, and thicker ice from deeper parts of the overdeepening is transported into locations previously occupied by thinner ice along the adverse slope, thickening the ice further (Fig. 6b, profile view); at the same time the constricted channels along the adverse slope cause an increase in water velocity that results in sediment erosion. So, while the glacier is accelerating, these two processes

TCD
8, 4463–4495, 2014

J. B. Turrin and R. R. Forster

(ice thickening and sediment erosion) are working in tandem to change the ratio of adverse slope to surface slope back below the supercooling threshold.

3. Eventually, the ratio of the angles of adverse slope to surface slope is reduced such that supercooling no longer occurs. When this happens the pressure-melting point has been sufficiently reduced along the adverse slope so that water traversing it has enough viscous energy to melt channel walls, expanding them (Fig. 6c, plan view). The expanded drainage channels allow efficient flow of water out of the overdeepening, de-pressurizing the distributed-cavity system and causing the till to consolidate, which causes the glacier to decelerate. This is the deceleration phase of the pulse. Deceleration reduces the compressive strain rate above the adverse slope and slows the transport of thicker ice up the adverse slope so that ice-thickening decreases, and eventually ceases, and surface ablation begins to thin the ice there (Fig. 6c, profile view). Meanwhile, the slower water flow of the de-pressurized drainage system allows sediment accumulation along the adverse slope. Eventually, ablation of the ice surface, and sediment deposition along the adverse slope, return the glacier to its pre-pulse geometry at the supercooling threshold, and the cycle repeats.

This model combines the processes of till transportation, erosion and deposition, basal hydraulics and thermodynamics, ice dynamics, surface ablation and glacier geometry in a chain of events that produces periodic ice motion in an overdeepening. In spite of the diversity of surface and subglacial processes that are incorporated into the model, it is primarily dependent upon climate and bedrock lithology. For instance, climate determines ice accumulation and ablation on the glacier surface, which in turn determines the rate at which the surface slope returns to its pre-pulse angle after supercooling stops; so climate helps determine the rate at which pulses cease. Accumulation and ablation rates also determine ice flux (ice thickness multiplied by the rate of ice flow) and the amount of melt water available to enter the subglacial hydraulic system, which combine to determine the rates of bedrock erosion, and sediment production

TCD
8, 4463–4495, 2014

and transport. Climate also influences the rate at which a pulse will achieve its peak by influencing strain thickening (velocity gradient multiplied by ice thickness) above the adverse slope. Greater strain thickening causes greater changes in surface slope and a more rapid end to supercooling. Bedrock lithology directly influences glacier geometry (width, thickness, and surface slope), which in turn affects glacier velocity, strain thickening, bedrock erosion, and sediment transport. Thus, bedrock lithology can influence where overdeepenings occur, the amount of till accumulation, deformation and erosion, the angle of the adverse slope, the supercooling threshold, and how rapidly pulses begin and end. In general, temperate glaciers with a high mass turnover (high snow accumulation in winter plus high ablation in summer), and a combination of valley configuration and bedrock lithology that produces an overdeepening, are most likely to pulse. Outside of southern Alaska, some regions that may have the requisite conditions include Patagonia, New Zealand, and Iceland.

5.6 Characteristics of non-pulsing glaciers

Of the 90 glaciers examined in this study, nine were positively identified as pulse-type, leaving 81 glaciers as either non-pulsing or possibly (but not positively) of pulse-type. As noted earlier, the pulsing glaciers have physical characteristics that suggest they are overdeepened at the location of the pulses, such as low surface slopes, and lateral constrictions or junctions with major tributaries. It is worthwhile to examine the non-pulsing glaciers to determine whether they have similar or different physical characteristics and compare them to the pulsing glaciers.

Fifty-three glaciers had velocity fields that were spatially or temporally too incomplete to identify pulses even if they did occur, so the physical characteristics of these glaciers were not examined. Clouds, cloud shadows, and a lack of suitable surface features to track were the main factors contributing to the incomplete velocity fields for these glaciers. A few glaciers are tidewater (Columbia, Harvard) or lake-calving (Knik) glaciers that appear to be moving too rapidly for pulsing to occur, so the physical characteristics of these glaciers were not examined because their behavior is determined by tidewater dynamics.

Eighteen glaciers had velocity fields of sufficient spatio-temporal density to identify pulses if they occurred, yet pulsing behavior was not observed on them. Of these 18 glaciers, six glaciers had none of the physical characteristics associated with an overdeepening. Seven of the 18 glaciers have junctions with major tributaries, but lack the shallow surface slope associated with an overdeepening where the tributary joins with the main glacier trunk. These glaciers widen their valleys to accommodate the additional ice flux from their tributaries, instead of deepening their valleys, so no overdeepenings are formed. The lone exception among this group of seven glaciers is Yentna Glacier, in the Central Alaska Range, which does not widen where tributaries join it in the upper ablation zone; instead the ice velocity steadily increases as one progresses down glacier to accommodate the additional ice flux from the tributaries. The increased ice velocity will cause Yentna Glacier to carve deeper into its valley, but the lack of any significant flattening of the surface slope suggests there is no overdeepening. Instead, Yentna Glacier probably has basal steps that coincide with each tributary. The medial moraines in the upper ablation zone of Yentna Glacier are not wavy, nor convolute, so it has no sign of past pulsing or surging behavior.

Five of the 18 glaciers with spatially and temporally dense velocity fields possessed both characteristics of overdeepenings, having either a lateral constriction or a major tributary, and a shallow surface slope at the same location. These glaciers are probably overdeepened, but they do not pulse. This could occur if the overdeepenings are not deep enough, or the ice not thick enough, to sufficiently depress the pressure-melting point and adequately supercool the basal water; consequently, the water will not freeze as it exits the overdeepening. The absence of pulsing behavior might also be due to an adverse slope so gently inclined that the pressure-melting point changes slowly enough along its length to allow viscous heating to warm the water fast enough to prevent freezing in the drainage channels. It is also possible the drainage system in an overdeepening is sufficiently isolated from the rest of the glacier such that the

TCD
8, 4463–4495, 2014

water pressure is never great enough to cause till dilation. This may happen when englacial drainage conduits bypass the overdeepening by going around or above the overdeepening, causing it to be hydraulically isolated (Fountain and Walder, 1998). Without sufficient water influx, the linked-cavity system within an overdeepening may never pressurize sufficiently to cause till dilation and the glacier will not pulse. It is also possible these five glaciers did pulse, but the pulses were not detected. As noted above, Black Rapids Glacier pulsed twice during the 1980s and 1990s (Nolan, 2003), but these pulses could not be detected in the velocity fields produced in this study, due to a lack of suitable surface features to track, occasionally patchy snow cover, clouds, and lack of available imagery during the 1990s. If the pulses of Black Rapids Glacier could not be detected using optical feature tracking, then it is possible other glaciers observed in this study also pulsed, but their pulses were not detected.

Of the 81 non-pulsing glaciers, six of them are suspected to have pulsed: Triumvirate Glacier and an unnamed glacier east of Barrier Glacier at 61°16′00″ N latitude, −152°5′21.89″ W longitude in the West Alaska Range, Trident Glacier in the East Alaska Range, Stephens Glacier and Tazlina Glacier in the Chugach Mountains, and an unnamed glacier in the Wrangell Mountains west of Copper Glacier at 62°6′55.01″ N latitude, −143°51′4.73″ W longitude. Each of these six glaciers has an obvious lateral constriction or junction with a major tributary, and all have an associated shallow surface slope indicating the presence of an overdeepening at the same location. The velocity fields for these six glaciers suggest they have pulsed, but their spatio-temporal velocity signatures are not sufficiently well-defined to positively identify pulsing behavior, therefore they were excluded from the group of nine pulsing glaciers discussed herein.

All glaciers presented in this study that definitely pulsed have obvious physical attributes indicating the presence of an overdeepening. All glaciers with spatially and temporally complete velocity fields and possessing only one, or zero, physical attributes of an overdeepening did not pulse. Eleven glaciers were identified with both characteristics of overdeepenings, but either they did not pulse, or their pulses could not be positively identified. So, it appears pulsing behavior requires a glacier to be overdeepened, but the presence of an overdeepening does not guarantee pulsing behavior.

5.7 Pulse synchronicity and climate

Four glaciers, Capps, Kahiltna, Matanuska, and Nabesna, all had pulses that peaked in 2001, while three glaciers, Kahiltna, Matanuska, and Ruth each had pulses that peaked in 2010, and two glaciers, Eldridge and Nizina, both had pulses that peaked in 2004 (Fig. 7). There appears to be some limited synchronicity of the pulse cycles among these nine glaciers across mountain ranges. Fowler and Schiavi (1998) suggest that synchronicity among surging ice streams of the Laurentide Ice Sheet (as proposed by Bond and Lotti, 1995) is not surprising because they are coupled via climate, and they note that even weakly coupled non-linear dynamic systems become synchronized. This same argument can be made for glaciers of southern Alaska; they are coupled by the predominant flow of weather patterns around the Gulf of Alaska. Even though glaciers further inland, such as in the Alaska Range, experience drier, colder conditions than those glaciers along the coast, they are still (perhaps weakly) coupled to glaciers along the coast, and thus over time they can synchronize with their counterparts to the south.

Considering the extent to which climate influences so many of the individual processes constituting the complete pulse mechanism described above, it should be no surprise that some limited synchronicity among pulsing glaciers exists. As an example of how annual meteorological conditions can influence the pulse cycle and cause synchronicity among glaciers, Positive Degree Days (PDDs) at the Talkeetna Airport (62.3° N, −150.1° W, 107.9 m a.s.l.) (http://www.ncdc.noaa.gov/oa/climate/ghcn-daily) were compared to the normalized velocity of the nine pulsing glaciers (Fig. 7). PDDs are a measure of the accumulated temperature above freezing at a location and are often used as a proxy for melt water production on the surface of a glacier. A peak in PDDs occurred in 2010, the same year pulses of Kahiltna, Matanuska, and Ruth glaciers peaked. These three glaciers were already in their acceleration phases, so additional melt water entering the glacier and reaching the base would enhance the process of till dilation and deformation, allowing the glacier to accelerate further, producing sufficient thickening of the ice such that the supercooling threshold is no longer surpassed. Thus, the pulse reaches its peak and the deceleration phase begins. The fact that four glaciers' pulses peaked in 2001, yet there is no obvious peak in PDDs that year, and the correlation between PDDs and the number of pulse peaks per year yields an R-squared value of 0.05, both indicate there are other unidentified variables that strongly influence pulse synchronization.

6 Conclusions

A systematic velocity survey of the largest glaciers of the Alaska Range, Chugach Mountains, and Wrangell Mountains in southern Alaska revealed nine glaciers that have pulsed within the past four decades. These nine glaciers, Capps, Copper, Eldridge, Kahiltna, Matanuska, Nizina, Nabesna, Ruth, and Sanford glaciers, have common characteristics where their pulses occurred. Each of them has shallow surface slopes in the range of 1 to 2°, and they are either constricted by their confining valleys or joined by a major tributary at these same locations, suggesting the pulses occur where the glaciers are overdeepened. Based on the idea that the glaciers are overdeepened, and incorporating a previous theory that says adverse slopes of glacier overdeepenings tend towards the supercooling threshold (Alley et al., 2003), a conceptual model to explain the cyclical behavior of pulsing glaciers is presented. The model accounts for the effects of glacier dynamics, ablation, and sediment transport to show that the pressure-melting point along an adverse slope oscillates above and below the supercooling threshold due to sediment accumulation and erosion and ice thickening and thinning. The effect of this oscillation is to periodically pressurize the subglacial drainage system sufficiently to allow the till to dilate and deform, causing the glacier to accelerate, followed by deceleration after supercooling ceases and the drainage system de-pressurizes, allowing the till to consolidate. The entire cycle typically lasts six to nine years and is controlled primarily by climate and bedrock lithology. The widespread existence of such pulsing glaciers, and the ease in which their behavior may be overlooked, suggests caution should be exercised when interpreting velocity changes over years or decades, because not all changes in glacier motion are a direct result of local meteorological conditions. Basal conditions can exert a greater influence on glacier dynamics than climate over the life of a pulse cycle.

Author contribution. J. B. Turrin performed all data analysis, developed the conceptual model of glacier motion through overdeepenings, and wrote the manuscript. R. R. FORSTER provided funding and oversight for this research, computer hardware and software for the data analysis, and edited the manuscript.

The Supplement related to this article is available online at doi:10.5194/tcd-8-4463-2014-supplement.

References

Alley, R. B., Lawson, D. E., Evenson, E. B., Strasser, J. C., and Larson, G. J.: Glaciohydraulic supercooling: a freeze-on mechanism to create stratified, debris-rich basal ice: II. Theory, J. Glaciol., 44, 563–569, 1998.

Alley, R. B., Lawson, D. E., Larson, G. J., Evenson, E. B., and Baker, G. S.: Stabilizing feedbacks in glacier-bed erosion, Nature, 424, 758–760, 2003.

Bond, G. C. and Lotti, R.: Iceberg discharges into the North Atlantic on millennial time scales during the last glaciations, Science, 267, 1005–1010, 1995.

Capps, S. R.: Glaciation on the north side of the Wrangell Mountains, Alaska, J. Geol., 18, 33–57, 1910.

Clarke, G. K. C.: Subglacial processes, Annu. Rev. Earth Pl. Sc., 33, 247–276, 2005.

Cook, J. S. and Swift, D. A.: Subglacial basins: their origin and importance in glacial systems and landscapes, Earth-Sci. Rev., 115, 332–372, 2012.

Creyts, T. T., Clarke, G. K. C., and Church, M.: Evolution of subglacial overdeepenings in response to sediment redistribution and glaciohydraulic supercooling, J. Geophys. Res.-Earth, 118, 423–446, 2013.

TCD

8, 4463–4495, 2014

Dow, C. F., Kavanaugh, J. L., Sanders, J. W., Cuffey, K. M., and MacGregor, K. R.: Subsurface hydrology of an overdeepened cirque glacier, J. Glaciol., 57, 1067–1078, 2011.

Evenson, E. B., Lawson, D. E., Strasser, J. C., Larson, G. J., Alley, R. B., Ensminger, S. L., and Stevenson, W. E.: Field Evidence for the Recognition of Glaciohydraulic Supercooling, edited by: Mickelson, D. M. and Attig, J. W., Geological Society of America, Boulder, CO., Special Paper, 337, 23–25, 1999a.

Evenson, E. B., Larson, G. J., Lawson, D. E., Alley, R. B., and Fleisher, P. J.: Observations of Glaciohydraulic Supercooling at the Bering and Malaspina Glaciers, Southeastern Alaska, Denver, Geol. Soc. Am. Abstr. with Prog, Vol. 30, p. 258, 1999b.

Evenson E. B., Lawson, D. E., Larson, G., Roberts, M., Knudsen, O., Russell, A. J., Alley, R. B., and Burkhart, P.: Glaciohydraulic supercooling and basal ice in temperate glaciers of Iceland, Geological Society of America Annual Meeting, 5–8 November 2001, Boston, paper 181-0, 2001.

Fitch, A. J., Kadyrov, A., Christmas, W. J., and Kittler, J.: Orientation correlation, British Machine Vision Conference, 2–5 September 2002, University of Cardiff, 133–142, 2002.

Fountain, A. G. and Walder, J. S.: Water flow through temperate glaciers, Rev. Geophys., 36, 299–328, 1998.

Fowler, A. C. and Schiavi, E.: A theory of ice-sheet surges, J. Glaciol., 44, 104–118, 1998.

Fowler, A. C., Murray, T., and Ng, F. S. L.: Thermally controlled glacier surging, J. Glaciol., 47, 527–538, 2001.

Frappé, T. and Clarke, G. K. C.: Slow surge of Trapridge Glacier, Yukon Territory, Canada, J. Geophys. Res., 112, F03S32, doi:10.1029/2006JF000607, 2007.

Goodwin, K., Loso, M. G., and Braun, M.: Glacial transport of human waste and survival of fecal bacteria on Mt. McKinley's Kahiltna Glacier, Denali National Park, Alaska, Arct. Antarct. Alp. Res., 44, 432–445, 2012.

Heid, T. and Kääb, A.: Evaluation of existing image matching methods for deriving glacier surface displacements globally from optical satellite imagery, Remote Sens. Environ., 118, 339–355, 2012.

Hooke, R. L. B.: Englacial and subglacial hydrology: A qualitative review, Arctic Alpine Res., 21, 221–233, 1989.

Hooke, R. L. B.: Principle of Glacier Mechanics, 2nd Edn., Cambridge University Press, Cambridge, UK, 429 pp., 2005.

Hooke, R. L. and Pohjola, V. A.: Hydrology of a segment of a glacier situated in an overdeepening, Storglaciären, Sweden, J. Glaciol., 40, 140–148, 1994.
Jansson, P.: Dynamics and hydrology of a small polythermal valley glacier, Geogr. Ann. A, 78, 171–180, 1996.
Kamb, B., Raymond, C. F., Harrison, W. D., Engelhardt, H., Echelmeyer, K. A., Humphrey, N., Brugman, M. M., and Pfeffer, T.: Glacier surge mechanism: 1982–1983 surge of Variegated Glacier, Alaska, Science, 227, 469–479, 1985.
Lawson, D. E., Strasser, J. C., Evenson, E. B., Alley, R. B., Larson, G. J., and Arcone, S. A.: Glaciohydraulic supercooling: a freeze-on mechanism to create stratified, debris-rich basal ice: I. Field evidence, J. Glaciol., 44, 547–562, 1998.
Leprince, S., Barbot, S., Ayoub, F. and Avouac, J. P.: Automatic and precise ortho-rectification, coregistration, and subpixel correlation of satellite images, application to ground deformation measurements, IEEE T. Geosci. Remote, 45, 1529–1558, 2007.
Li, S., Benson, C., Gens, R., and Lingle, C.: Motion patterns of Nabesna Glacier (Alaska) revealed by interferometric SAR techniques, Remote Sens. Environ., 112, 3628–3638, 2008.
March, R. S., Mayo, L. R., and Trabant, D. C.: Snow and ice volume on Mount Spurr Volcano, Alaska, 1981, US Geological Survey Water-Resources Investigations Report 97-4142, 41 pp., 1997.
Mayo, L. R.: Identification of unstable glaciers intermediate between normal and surging glaciers. Academy of Sciences of the USS R. Section of Glaciology of the Soviet Geophysical Committee and Institute of Geography, Data of Glaciological Studies Chronicle, Discussion, 133, 133–135, Moscow, May 1978, 1978.
Murray, T., Strozzi, T., Luckman, A., Jiskoot, H., and Christakos, P.: Is there a single surge mechanism? Contrasts in dynamics between glacier surges in Svalbard and other regions, J. Geophys. Res., 108, 2237, doi:10.1029/2002JB001906, 2003.
Nolan, M.: The “Galloping Glacier” trots: decadal-scale speed oscillations within the quiescent phase, Ann. Glaciol., 36, 7–13, 2003.
Penck, A.: Glacial features in the surface of the Alps, J. Geol., 13, 1–19, 1905.
Post, A.: Distribution of surging glaciers in western North America, J. Glaciol., 8, 229–240, 1969.
Richter, D. H., Preller, C. C., Labay, K. A., and Shew, N. B.: Geologic Map of the Wrangell-Saint Elias National Park and Preserve, Alaska, US Geological Survey Scientific Investigations Map 2877, 2006.

TCD
8, 4463–4495, 2014
A conceptual model of cyclical glacier flow in overdeepenings
J. B. Turrin and R. R. Forster

Truffer, M., Harrison, W. D., and Echelmeyer, K. A.: Glacier motion dominated by processes deep in underlying till, J. Glaciol., 46, 213–221, 2000.
Turrin, J. B., Forster, R. R., Larsen, C., and Sauber, J.: The propagation of a surge front on Bering Glacier, Alaska, 2001–2011, Ann. Glaciol., 54, 221–228, 2013.
Turrin, J. B, Forster, R. R., Sauber, J. M., Hall, D. K. and Bruhn, R. L.: Effects of bedrock lithology and subglacial till on the motion of Ruth Glacier, Alaska, deduced from five pulses from 1973–2012, J. Glaciol., accepted, 2014.
Ward, J. D., Anderson, R. S., and Haeussler, P. J.: Scaling the Teflon Peaks: Rock type and the generation of extreme relief in the glaciated western Alaska Range, J. Geophys. Res., 117, F01031, doi:10.1029/2011JF002068, 2012.
Willis, I. C.: Intra-annual variations in glacier motion: a review, Prog. Phys. Geog., 19, 61–106, 1995.
Wilson, F. H., Dover, J. H., Bradley, D. C., Weber, F. R., Bundtzen T. K., and Haeussler, P. J.: Geologic Map of Central (Interior) Alaska, US Geological Survey Open-File Report OF 98-133, 1998.

TCD
8, 4463–4495, 2014
A conceptual model of cyclical glacier flow in overdeepenings
J. B. Turrin and R. R. Forster

Title Page
Abstract Introduction
Conclusions References
Tables Figures
◀ ▶
Back Close
Full Screen / Esc
Printer-friendly Version
Interactive Discussion

Table 1. Landsat images used to produce velocity fields for the Wrangell Mountains.

Path/Row	Date 1	Sensor	Path/Row	Date 2	Sensor
WRS1 71/16	24 Sep 1972	MSS 1	WRS1 71/16	19 Sep 1973	MSS 1
WRS1 71/16	19 Sep 1973	MSS 1	WRS1 71/17	4 Jul 1974	MSS 1
WRS1 71/17	4 Jul 1974	MSS 1	WRS1 71/16	8 Jul 1975	MSS2
WRS1 71/16	8 Jul 1975	MSS 2	WRS1 71/16	25 Aug 1976	MSS 2
WRS1 71/16	25 Aug 1976	MSS 2	WRS1 71/16	20 Aug 1977	MSS 2
WRS1 71/16	20 Aug 1977	MSS 2	WRS1 71/16	10 Jul 1978	MSS 2
WRS1 71/16	10 Jul 1978	MSS 2	WRS1 71/16	19 Aug 1979	MSS 3
WRS1 71/16	15 May 1980	MSS 3	WRS1 71/16	1 May 1981	MSS 2
WRS1 71/16	17 Aug 1981	MSS 2	WRS2 65/17	12 Aug 1982	MSS 4
WRS2 65/17	12 Aug 1982	MSS 4	WRS2 65/17	16 Sep 1983	MSS 4
WRS2 65/17	25 Apr 1983	MSS 4	WRS2 65/17	5 May 1984	MSS 5
WRS2 65/17	5 May 1984	MSS 5	WRS2 65/17	22 Apr 1985	MSS 5
WRS2 65/17	27 Jul 1985	TM 5	WRS2 65/17	16 Sep 1986	TM 5
WRS2 65/17	16 Sep 1986	TM 5	WRS2 65/17	2 Aug 1987	TM 5
WRS2 65/17	2 Aug 1987	TM 5	WRS2 65/17	12 Aug 1988	TM 4
WRS2 65/17	7 Jul 1995	TM 5	WRS2 65/17	23 Jun 1996	TM 5
WRS2 65/17	23 Jun 1996	TM 5	WRS2 65/17	29 Aug 1997	TM 5
WRS2 65/17	29 Aug 1997	TM 5	WRS2 65/17	29 Jun 1998	TM 5
WRS2 65/17	29 Jun 1998	TM 5	WRS2 65/17	2 Jul 1999	TM 5
WRS2 65/17	29 Apr 1999	TM 5	WRS2 65/17	9 May 2000	TM 5
WRS2 65/17	9 May 2000	TM 5	WRS2 65/17	12 May 2001	ETM+7
WRS2 65/17	15 Jul 2001	ETM+7	WRS2 65/17	3 Aug 2002	ETM+7
WRS2 65/17	3 Aug 2002	ETM+7	WRS2 65/17	6 Aug 2003	ETM+7
WRS2 65/17	6 Aug 2003	ETM+7	WRS2 65/17	16 Aug 2004	TM 5
WRS2 65/17	16 Aug 2004	TM 5	WRS2 65/17	11 Aug 2005	ETM+7
WRS2 65/17	11 Aug 2005	ETM+7	WRS2 65/17	13 Jul 2006	ETM+7
WRS2 65/17	8 Apr 2006	ETM+7	WRS2 65/17	26 Mar 2007	ETM+7
WRS2 65/17	17 Aug 2007	ETM+7	WRS2 65/17	11 Aug 2008	TM 5
WRS2 65/17	11 Aug 2008	TM 5	WRS2 65/17	29 Jul 2009	TM 5
WRS2 65/17	29 Jul 2009	TM 5	WRS2 65/17	18 Sep 2010	TM 5
WRS2 65/17	21 May 2010	ETM+7	WRS2 65/17	24 May 2011	ETM+7
WRS2 65/17	12 Aug 2011	ETM+7	WRS2 65/17	14 Aug 2012	ETM+7
WRS2 65/17	8 Apr 2012	ETM+7	WRS2 65/17	21 May 2013	OLI 8

TCD
8, 4463–4495, 2014

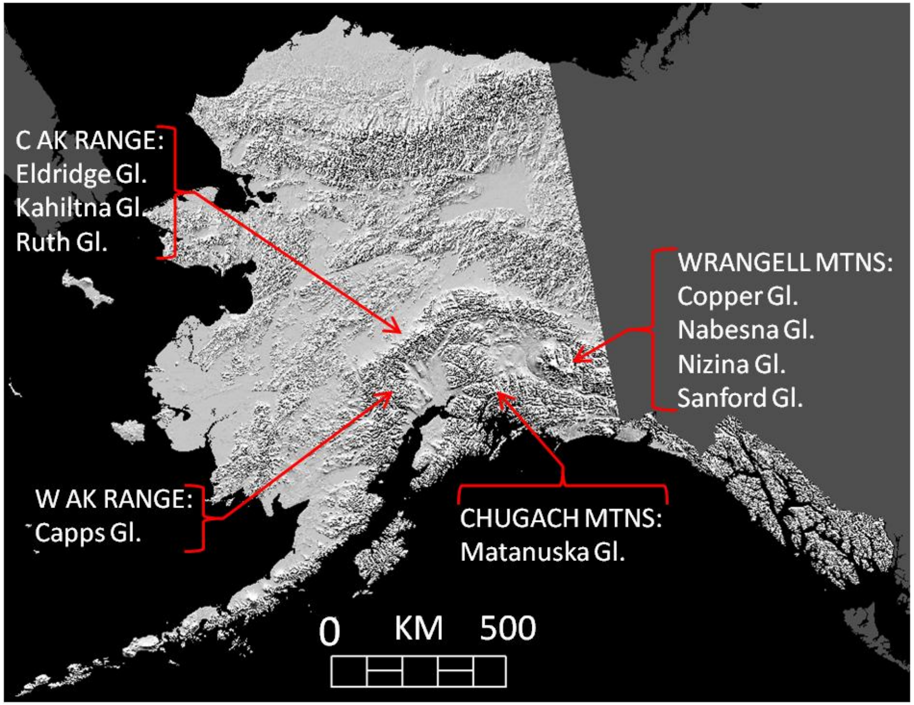

Figure 1. Location of pulsing glaciers in this study and the mountain ranges of southern Alaska that contain them.

TCD
8, 4463–4495, 2014

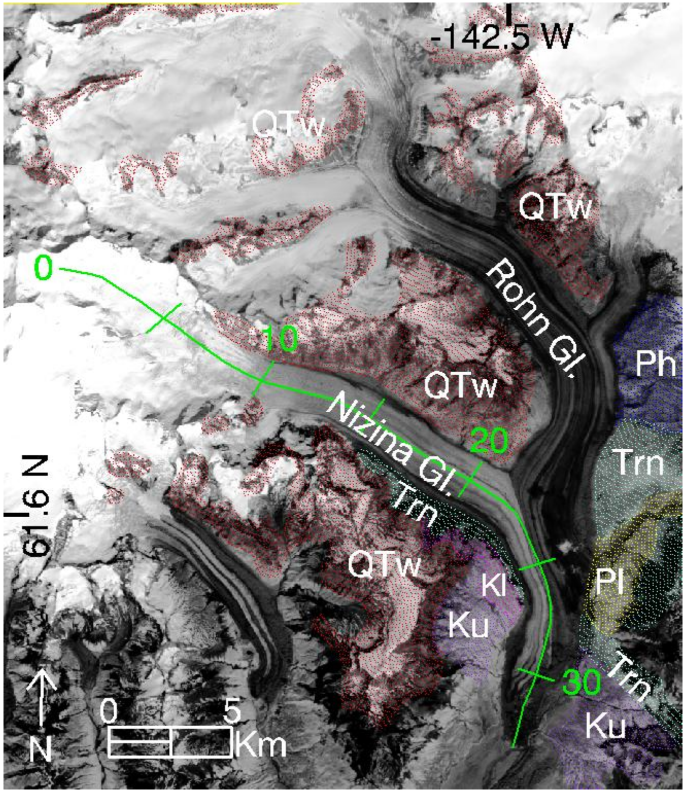

Figure 2. Nizina Glacier. Transect along glacier centerline (shown in green) indicates the location of the velocity profiles shown in Fig. 5, units are km. Areas highligted in red (QTw) or aqua (Trn) indicate areas underlain by crystalline bedrock composed of lava. Areas highlighted in magenta (Kl), purple (Ku), yellow (Pl), or blue (Ph) indicate areas underlain by sedimentary bedrock (Richter et al., 2006).

TCD
8, 4463–4495, 2014

A conceptual model of cyclical glacier flow in overdeepenings

J. B. Turrin and R. R. Forster

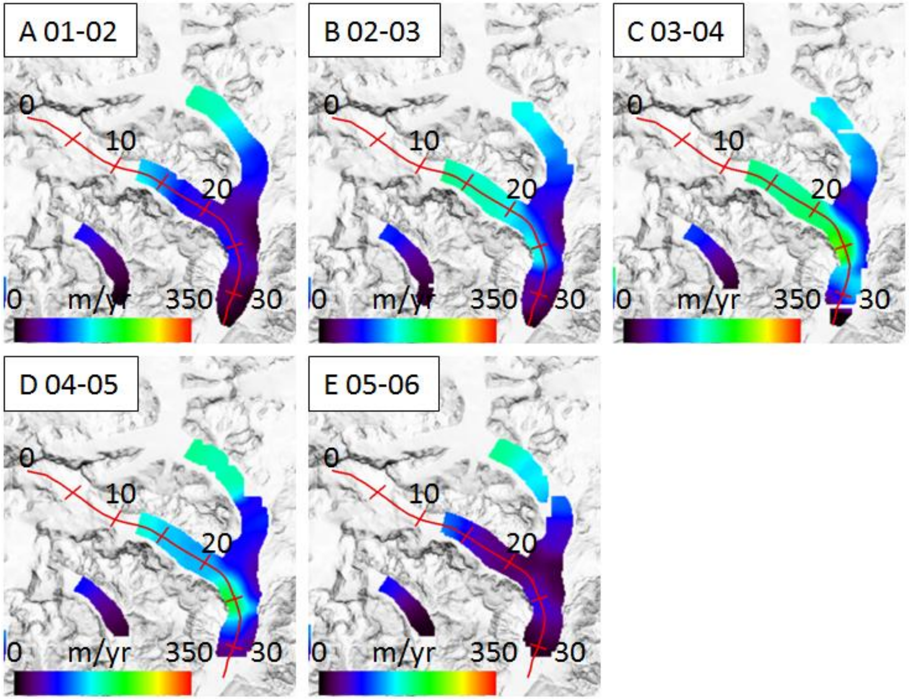

Figure 3. Velocity fields for Nizina Glacier encompassing its pulse from 2001–2002 to 2005–2006. **(a)** 2001–2002 velocity. **(b)** 2002–2003 velocity. **(c)** 2003–2004 velocity. **(d)** 2004–2005 velocity. **(e)** 2005–2006 velocity. Velocity fields from 2006–2007 to 2012–2013 are not shown.

TCD
8, 4463–4495, 2014

A conceptual model of cyclical glacier flow in overdeepenings

J. B. Turrin and R. R. Forster

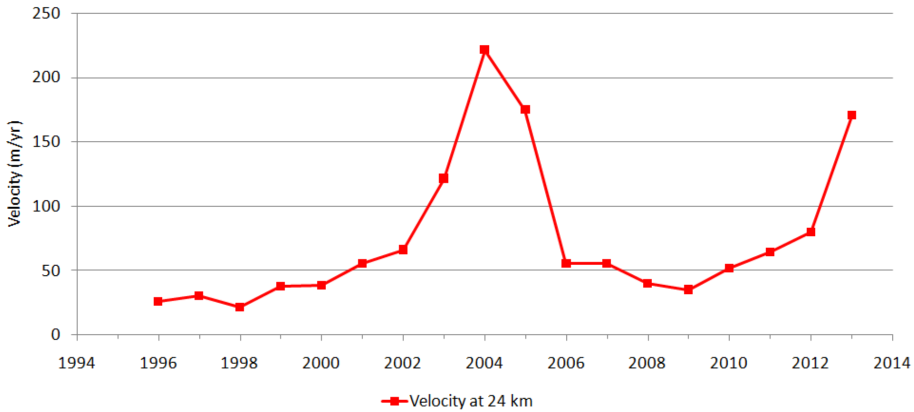

Figure 4. Velocity of Nizina Glacier through time, at 24 km. One complete pulse cycle is seen, with a peak in 2004 of 221.1 m a^{-1}, and the acceleration phase of a second pulse is seen, with its current peak in 2013 of 170.3 m a^{-1}.

TCD
8, 4463–4495, 2014

A conceptual model of cyclical glacier flow in overdeepenings

J. B. Turrin and R. R. Forster

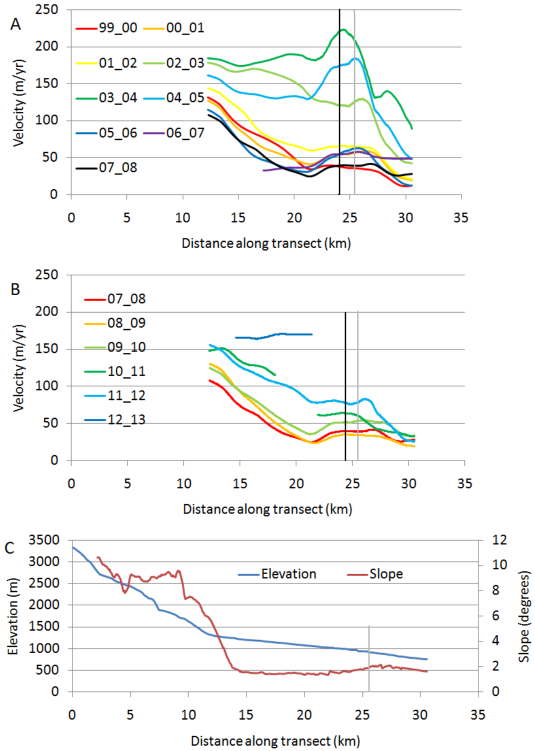

Figure 5. Centerline profiles for Nizina Glacier. **(a)** Velocity profiles from 1999–2000 to 2007–2008 showing the first pulse. **(b)** Velocity profiles from 2007–2008 to 2012–2013 showing the acceleration phase of the second pulse. **(c)** Elevation and slope of the glacier surface. Vertical black line at 24 km in **(a)** and **(b)** indicates position at which velocity values were taken to create time-series in Fig. 4. Vertical gray line at 26 km indicates location of major change in bedrock lithology.

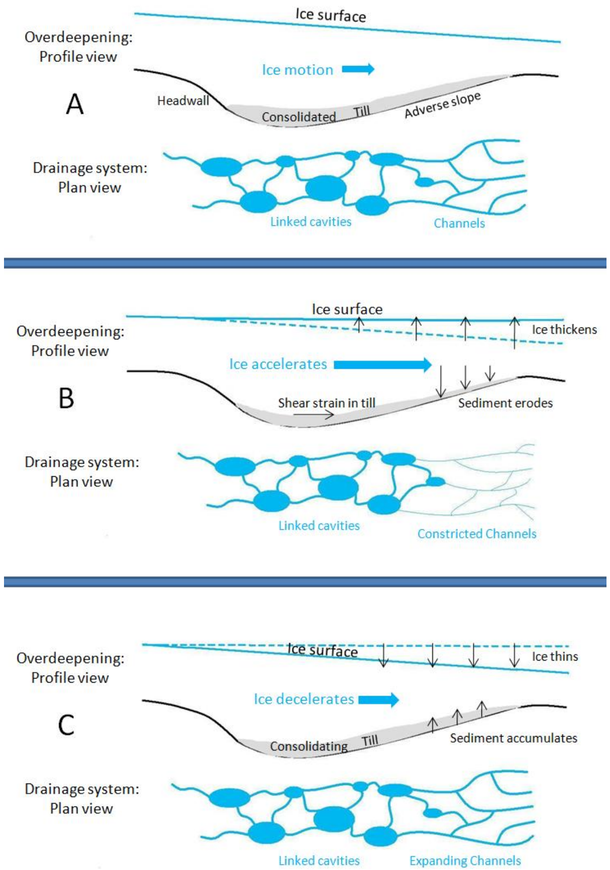

Figure 6. Illustration of the physical mechanisms which cause glacier pulses. **(a)** Initial conditions. **(b)** Acceleration phase **(c)** Deceleration phase. See Sect. 5.5 for complete description.

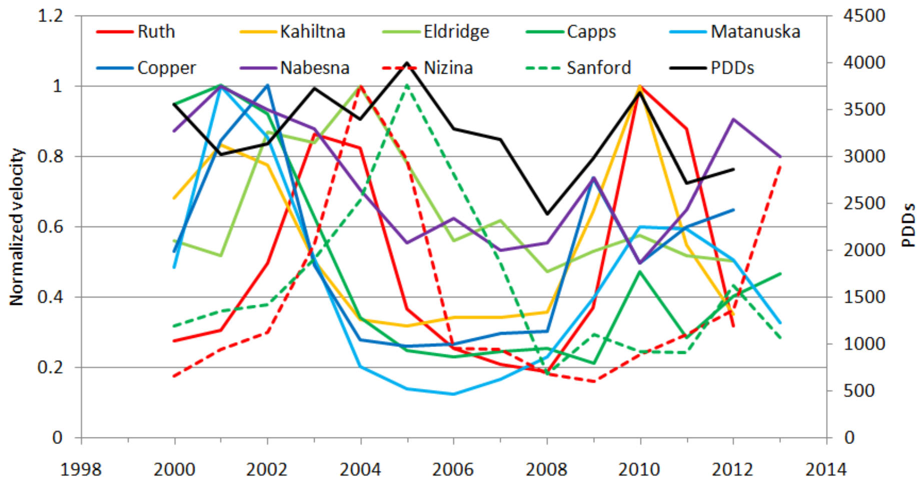

Figure 7. Normalized velocity of nine pulsing glaciers and Positive Degree Days (PDDs). Four pulses peaked in 2001 (Capps, Matanuska, Kahiltna, Nabesna); three pulses peaked in 2010 (Kahiltna, Matanuska, Ruth) and Capps Gl. had a spike in velocity this same year; two pulses peaked in 2004 (Eldridge, Nizina). The coincident peaks suggest synchronicity between glaciers that exist within the same regional climate. The simultaneous peak of PDDs and three pulsing glaciers in 2010 illustrates the influence annual meteorological conditions can have on the pulse cycle by causing glaciers currently in the acceleration phase of a pulse to peak.

TCD
8, 4463–4495, 2014